COMPARATIVE SOIL EROSION SUSCEPTIBILITY ASSESSMENT USING STATISTICAL AND DATA-DRIVEN TECHNIQUES: EVIDENCE FROM THE CHARTAK DISTRICT, UZBEKISTAN

KHOLMURODOVA, M.[1*] – JULIEV, M.[1,2,3] – KHAMIDULLAEV, SH.[4] – DJANPULATOVA, Z.[1] – TURDALIEVA, S.[1] – KHADJIEVA, Z.[1] – ABDIKAIROV, B.[5] – SHAMSIEV, M.[1] – KHAKBERDIEV, O.[4]

[1]*Institute of Fundamental and Applied Research, "TIIAME" National Research University, Kori Niyoziy 39A, Tashkent 100000, Uzbekistan*
(e-mails: zilolakhondjanpulatova@gmail.com; sojidabonuturdalieva@gmail.com; zuhraxadjiyeva955@gmail.com; shamsiyevmurodjon007@gmail.com)

[2]*Turin Polytechnic University in Tashkent, Little Ring Road Street 17, 100095 Tashkent, Uzbekistan*
(e-mail: mukhiddinjuliev@gmail.com)

[3]*Tashkent State Technical University, Universitet 2, Tashkent 100095, Uzbekistan*

[4]*"TIIAME" National Research University, Kori Niyoziy 39A, Tashkent 100000, Uzbekistan*
(e-mail: shohjahon1208@tiiame.uz; o.xakberdiyev@tiiame.uz)

[5]*Institute of Agriculture and Agrotechnologies of Karakalpakstan, Abdametov Street, Nukus 230109, Uzbekistan*
(e-mail: abdikairovbekmurat12@gmail.com)

**Corresponding author*
e-mail: kholmurodovamadinabonu1@gmail.com

(Received 17th Sep 2025; accepted 5th Dec 2025)

Abstract. Soil erosion is a significant environmental problem that negatively affects agriculture and land resources. This study aimed to evaluate soil erosion susceptibility using Geographic Information Systems (GIS) and three bivariate statistical models: Statistical Index (SI), Frequency Ratio (FR), and Certainty Factor (CF). A total of 133 erosion points within the study area were used as reference data. Remote sensing and topographic datasets were used to derive nine widely applied environmental conditioning factors slope, aspect, plan curvature, elevation, stream power index (SPI), drainage density, distance to rivers, normalized difference vegetation index (NDVI), and land use/land cover (LULC). These factors were selected based on their frequent use and proven effectiveness in recent erosion-susceptibility studies. Raster layers with a resolution of 30 m were produced for each factor. The susceptibility maps indicated that large portions of the study area fall within the high to very high susceptibility categories. This is especially true for rangelands, steep slopes, areas with sparse vegetation. Quantitative validation using the Area Under the Receiver Operating Characteristic Curve (ROC–AUC) indicated acceptable predictive performance: 0.879 for SI, 0.843 for FR, and 0.878 for CF. The SI (0.879) and CF (0.878) models yielded the highest AUC values, whereas the FR model produced a lower value (0.843). All three models demonstrated strong predictive capability based on ROC–AUC metrics. Overall, the results underscore the importance of integrating both statistical models and GIS techniques to assess soil erosion susceptibility. The generated maps can help decision-makers develop soil conservation strategies, prioritize high-risk areas, and promote sustainable land use.
Keywords: *soil erosion, susceptibility mapping, statistical index, frequency ratio, certainty factor, GIS, AUC/ROC*

Introduction

Soil erosion is one of the most significant environmental problems of the 21st century. It leads to severe land degradation, loss of soil fertility, and ultimately affects global food

http://www.aloki.hu ● ISSN 1589 1623 (Print) ● ISSN 1785 0037 (Online)
DOI: http://dx.doi.org/10.15666/aeer/2401_11131131

security (Arabameri et al., 2018, 2019b; Kholmurodova et al., 2025b). Global assessments indicate that approximately one-third of the world's soils are currently degraded, and projections suggest that up to 90% may be degraded by 2050 if appropriate measures are not implemented (Montanarella et al., 2016). Among various degradation processes, soil erosion is considered the most damaging (Juliev et al., 2024a), as it removes nutrient-rich topsoil essential for agricultural productivity, ecosystem functioning, and carbon storage (Arabameri et al., 2021; David Raj et al., 2025; Schmidt, 2000; Zachar, 1982). This process not only reduces crop yields but also increases sediment accumulation in rivers and reservoirs, deteriorates water quality, and contributes to long-term risks of desertification (Bouamrane et al., 2024; Kanianska et al., 2024).

In dry and semi-dry regions, soil erosion presents a particularly serious challenge because fragile ecosystems are highly sensitive to external disturbances (Borges Neto et al., 2023; Djanpulatova et al., 2025; Vaezi and Sahandi, 2024). Uzbekistan and other parts of Central Asia are among the most erosion-prone areas due to their harsh continental climate, rapid agricultural development, and widespread unsustainable land-use practices (Abdikairov et al., 2024; Gafurova and Juliev, 2021; Juliev et al., 2022). Overgrazing, monocropping, deforestation, and poor irrigation management have accelerated erosion rates in the region. Soil erosion already affects large areas of agricultural land in Uzbekistan, posing a serious threat to national food security and the livelihoods of rural communities (Juliev et al., 2024; Sodikova et al., 2025). Recent studies reveal that erosion processes in the country are intensifying, making reliable erosion-risk assessments both urgent and necessary (Kholdorov et al., 2023).

To address these issues, researchers worldwide increasingly apply geospatial technologies such as Remote Sensing (RS) and GIS to monitor, analyze, and predict erosion processes (Borrelli et al., 2021). RS enables the acquisition of surface information from satellite and aerial imagery, facilitating the observation of landscape changes over time (Wang et al., 2024). Meanwhile, GIS provides an effective platform for storing, integrating, and analyzing spatial datasets, allowing comprehensive and spatially explicit evaluations of erosion dynamics and their influencing factors (Samuel et al., 2025). The integration of RS and GIS has become essential for modern erosion-susceptibility mapping and environmental risk assessment (Allafta and Opp, 2022).

Alongside geospatial approaches, numerous statistical and data-driven models have been developed and widely applied to map erosion susceptibility (Raza et al., 2024). These models establish relationships between erosion occurrences and conditioning factors (Arabameri et al., 2020b), making it possible to estimate susceptibility levels across landscapes (Arabameri et al., 2019). Comparative studies from various regions confirm their effectiveness in producing accurate susceptibility maps (Akgün and Türk, 2011; Bouamrane et al., 2024), although model performance often varies depending on local environmental conditions and data availability (Borrelli et al., 2021).

In Uzbekistan, soil erosion has been studied at multiple spatial scales, mainly using the Revised Universal Soil Loss Equation (RUSLE) and remote-sensing techniques. RUSLE has been applied in the Bekabad and Parkent districts (Ibragimov et al., 2024), and in the Ugam–Chatkal National Park (Juliev et al., 2024), to estimate annual soil loss and examine the effects of topography and land cover. Rainfall erosivity under future climate scenarios has been assessed in the Chirchik–Akhangaran catchment (Gafforov et al., 2020). In the Aral Sea region, studies have investigated wind-erosion risks using modeling and InSAR technologies (Chen et al., 2025). Field-based research in the Namangan region has examined soil-conservation practices such as terracing and mulching (Koriyev et al., 2024b).

http://www.aloki.hu ● ISSN 1589 1623 (Print) ● ISSN 1785 0037 (Online)
DOI: http://dx.doi.org/10.15666/aeer/2401_11131131

Despite these efforts, most erosion-related studies in Uzbekistan have focused on estimating annual soil loss using RUSLE or analyzing erosion processes at regional and basin scales (Juliev et al., 2024; Koriyev et al., 2024). While these approaches provide valuable information, they do not sufficiently reflect spatial variations in erosion susceptibility at lower administrative levels. In particular, district-level susceptibility mapping supported by statistical models has not yet been undertaken in the country.

To address this gap, the present study focuses on the Chartak district of the Namangan region, situated in the southern foothills of the Chatkal mountain range and highly susceptible to erosion due to its topographic and climatic characteristics. Within the ArcGIS 10.6.1 environment, three commonly used statistical models were applied to generate erosion-susceptibility maps and evaluate their performance. This study represents the first application of such comparative modeling in Uzbekistan and aims to provide essential guidance for sustainable soil and land management planning.

Materials and methods

Study area

Chartak is a district located in the Namangan region of Uzbekistan, situated in the southern foothills of the Chatkal Range. The district covers approximately 0.36 thousand km². Elevation increases from south to north, ranging from about 400 to 1300 m above sea level, and the terrain is predominantly flat to moderately hilly (Koriyev et al., 2024b). The district lies within a subtropical climatic zone, characterized by hot and dry summers and relatively mild winters. According to the Climate Hazards Group InfraRed Precipitation with Stations (CHIRPS), TerraClimate high-resolution global climate dataset (TerraClimate), and the ECMWF ERA5-Land reanalysis dataset (ERA5-Land), the climate of Chartak shows pronounced interannual variability rather than a stable average regime. Annual precipitation totaled 225–260 mm in 2000, increased to 319–348 mm in 2010, declined sharply to 148–183 mm in 2020, and partially recovered to 179–254 mm in 2024. This alternating sequence of wet (2010) and dry (2020) periods reflects the region’s increasing climatic instability, which affects soil-moisture dynamics, runoff generation, and erosion intensity. Mean annual temperature also fluctuated significantly during the same period: 5–13°C in 2000, 7–13°C in 2010, 6–12°C in 2020, and 8–15°C in 2024. The cooling phase observed in 2020, followed by resurgence of warmer conditions in 2024, demonstrates the sensitivity of the region to broader climatic shifts. These temperature changes, combined with variable precipitation, directly influence vegetation growth, evapotranspiration rates, and the severity of sheet and rill erosion, particularly under intensive irrigation practices. Climatic conditions vary with elevation, being hotter and drier in the lowlands and cooler and wetter in the mountainous areas. The dominant soil types in the district are gray soils, and agricultural development is actively expanding in the area (Koriyev et al., 2024b). Furthermore, official assessments indicate that the geological and topographic characteristics of Chartak increase its susceptibility to natural hazards such as landslides and floods (World Bank, 2019). *Figure 1* presents the geographical location of the study area.

Soil characteristics

The soils in the study area exhibit substantial variation due to geomorphological conditions and long-term agricultural activities (Koriyev et al., 2024b). The most

http://www.aloki.hu ● ISSN 1589 1623 (Print) ● ISSN 1785 0037 (Online)
DOI: http://dx.doi.org/10.15666/aeer/2401_11131131

common soil types are irrigated sierozems, including dark, typical, and light variants. In addition, meadow-sierozem, meadow, gray-brown, and alluvial soils occur in certain parts of the district (Rustamjonovich, 2019). The soils are predominantly loamy, although gravel or crushed-stone layers are frequently present at depths of 30–100 cm. Organic matter content remains low, with humus levels ranging from 0.3% to 2.8%. Nitrogen and phosphorus concentrations are generally low to moderate, whereas potassium levels are comparatively higher. Salinity is not widespread; however, slight salinization and signs of irrigation-induced erosion can be observed in some areas (Koriyev et al., 2024a). Light sierozems and meadow soils collectively occupy more than two-thirds of the total territory, forming the primary soil resource base for agricultural production (Sanakulov et al., 2023). These soil characteristics indicate both opportunities and limitations for sustainable land management within the district. Similar soil conditions have been documented in other parts of Central Asia, suggesting that the study area is representative of regional soil formation patterns influenced by arid climatic conditions and irrigation practices (Dou et al., 2022). Field observations confirmed the presence of erosion processes in the region. *Figure 2* illustrates selected erosion points within the study area.

Methodology

This study employed a multi-stage methodological framework (*Fig. 3*). To ensure a systematic workflow, the analysis was divided into four main steps: data preparation, factor derivation, modeling, and validation. First, Google Earth (GE) was used to identify 133 erosion points across the study area and to develop an erosion inventory map. This inventory served as the dependent variable for subsequent susceptibility modeling.

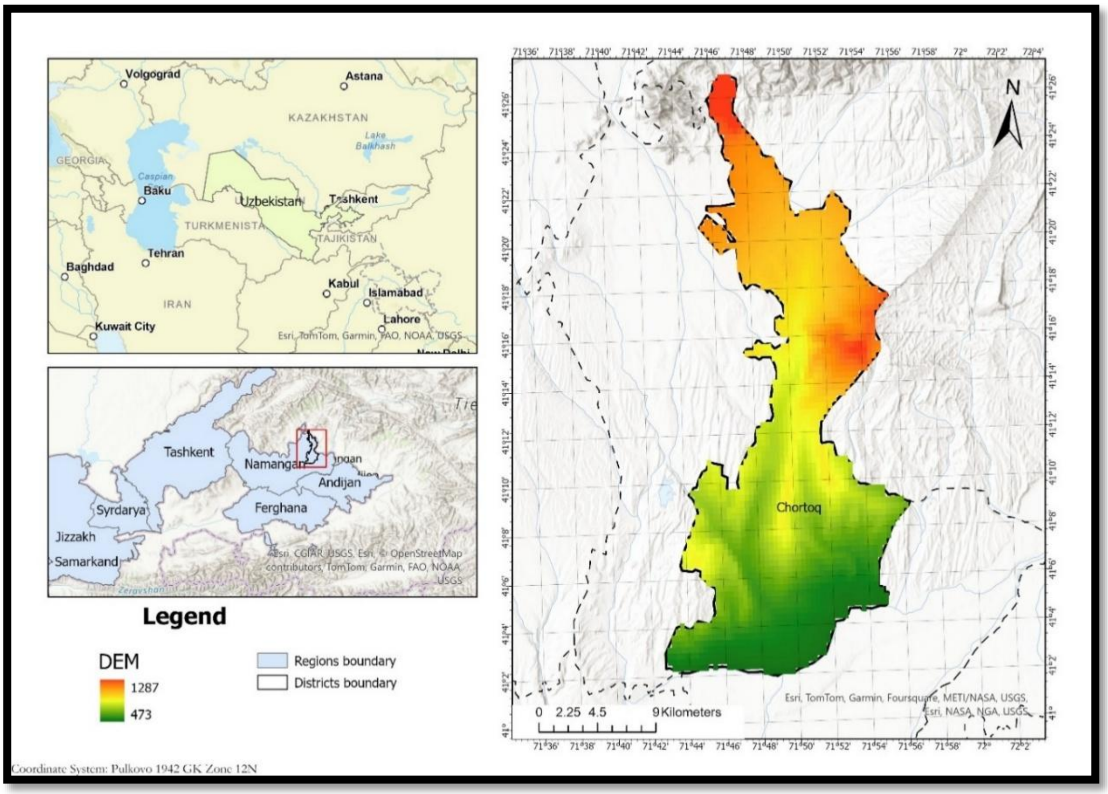

***Figure 1.** Location of study area*

http://www.aloki.hu ● ISSN 1589 1623 (Print) ● ISSN 1785 0037 (Online)
DOI: http://dx.doi.org/10.15666/aeer/2401_11131131

Figure 2. *Field photographs illustrating soil erosion features observed in the study area*

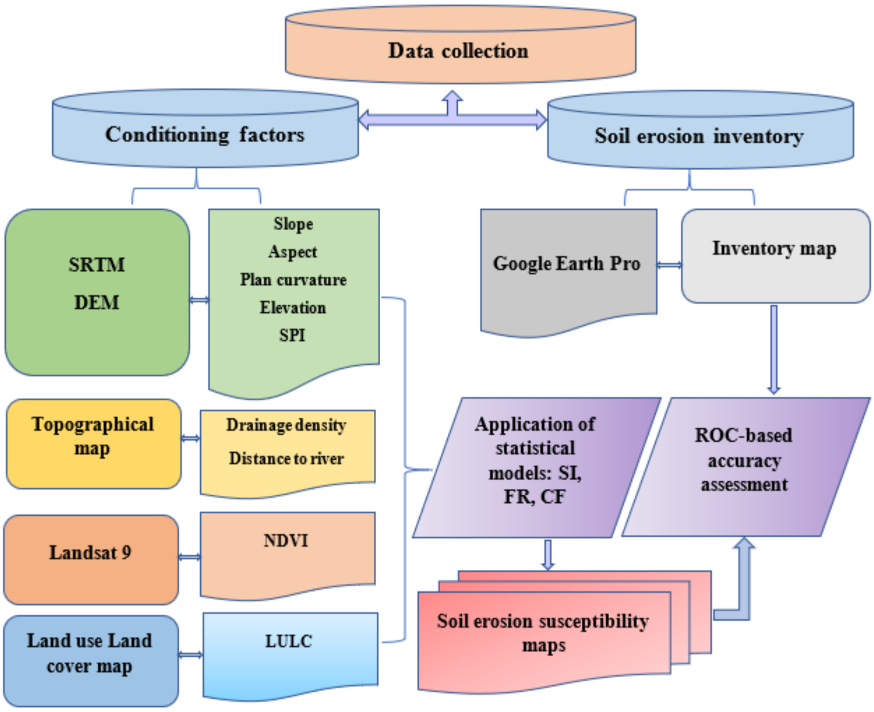

Figure 3. *Flowchart of research*

Because erosion features in the Chartak district occur predominantly in steep rangeland areas, the mapped erosion points are naturally unevenly distributed across the landscape. Flat cropland areas in the northern part of the district showed no visible erosion features and therefore contained no reference points. Since the SI, FR, and CF models rely on pixel-based ratios of erosion and non-erosion areas rather than uniform spatial sampling, this uneven distribution does not affect model representativeness and is consistent with standard practices in erosion-susceptibility mapping.

Second, nine widely used environmental conditioning factors were derived from existing geospatial datasets rather than created as new indicators (Kholmurodova et al., 2025a). The selected factors included slope, aspect, plan curvature, elevation, drainage density, SPI, distance to rivers, NDVI, and LULC (*Table 1*). These variables were produced in ArcGIS 10.6.1 using data from the Shuttle Radar Topography Mission Digital Elevation Model (SRTM DEM), Landsat 8 imagery, topographic maps, and other available sources. To ensure comparability, all factor layers were standardized to a spatial resolution of 30 m and projected into a uniform coordinate system. Third, three commonly applied bivariate statistical models SI, FR, and CF were used to quantify the relationships between erosion occurrences and classes of conditioning factors. The modeling procedures were performed in ArcGIS 10.6.1, and the resulting factor weightings were converted into raster layers to produce soil-erosion susceptibility maps. Finally, the predictive performance of the susceptibility maps was evaluated using the AUC-ROC. ROC curves and AUC values were generated using the ArcSDM toolbox in ArcGIS, providing an objective assessment of model accuracy and enabling comparison among the applied methods. This structured methodology ensured transparency, reproducibility, and adherence to commonly accepted best practices for erosion-susceptibility assessment.

Table 1. *List of factors used for soil erosion susceptibility maps*

Factor	Source	Resolution	Classes	Method	References
Slope	SRTM DEM	30 m	1. <2.8, 2. 2.8-5.6, 3. 5.6-9.1, 4. 9.1-13.6, 5. 13.6-20.9, 6. >20.9	Natural break	Arabameri et al. (2019b)
Aspect	SRTM DEM	30 m	1. F, 2. N, 3. NE, 4. E, 5. SE, 6. S, 7. SW, 8. W, 9. NW, 10. N	Equal interval	Esmali Ouri et al. (2020)
Plan curvature	SRTM DEM	30 m	1. Concave, 2. Flat, 3. Convex	Manual	Arabameri et al. (2020a)
Elevation	SRTM DEM	30 m	1. <586, 2. 586-709, 3. 709-839, 4. 839-979, 5. >979	Natural break	Arabameri et al. (2019b)
NDVI	Landsat 9	30 m	1. <0.14, 2. 0.14-0.23, 3. >0.64	Natural break	Arabameri et al. (2020a)
Distance to river	Topographical map	1:50,000	1. <600, 2. 600-1329, 3. 1329-2168, 4. 2168-3380, 5. >3380	Manual	Arabameri et al. (2020a)
LULC	Land use map	1:100,000	1. Water, 2. Tree, 3. Crops, 4. Build, 5. Bareland, 6. Rangeland	Land use type	–
SPI	SRTM DEM	30 m	1. <0, 2. 0-0.61, 3. 0.61-1.39, 4. 1.39-2.49, 5. >2.49	Natural break	Arabameri et al. (2019c)
Drainage density	Topographical map	1:50,000	1. <0.68, 2. 0.68-1.99, 3. 1.99-3.20, 4. >3.20	Manual	Arabameri et al. (2019c)

Conditioning factors

Topographic, hydrological, vegetation-related, and land-use characteristics collectively influence the occurrence and intensity of soil erosion (Arabameri et al., 2019a). Elevation reflects the vertical variability of the terrain and affects the potential for soil detachment and transport processes (Esmali Ouri et al., 2020). Slope is a critical

http://www.aloki.hu ● ISSN 1589 1623 (Print) ● ISSN 1785 0037 (Online)
DOI: http://dx.doi.org/10.15666/aeer/2401_11131131

factor governing runoff velocity and infiltration capacity; steeper slopes generally correspond to higher erosion rates due to increased surface runoff (Wang et al., 2023). Aspect, which describes the orientation of slope surfaces, and plan curvature, which indicates whether the terrain is concave or convex, both influence the direction and concentration of overland flow and, consequently, erosion patterns (Meliho et al., 2018; Arabameri et al., 2019a). Hydrological indices such as the SPI and drainage density quantify the erosive energy of surface water and the efficiency of runoff pathways within the landscape (Esmali Ouri et al., 2020; Meshram et al., 2022). Proximity to rivers also affects how rapidly runoff reaches channel systems, thereby influencing the initiation of erosion processes (Arabameri et al., 2020a). Vegetation-related factors including the NDVI and LULC conditions provide insight into the protective capacity of surface cover. Higher vegetation density generally reduces erosion hazards by decreasing runoff velocity and enhancing soil stability (Cao et al., 2023). Collectively, these conditioning factors offer a comprehensive understanding of the spatial variability and susceptibility of soil erosion within the study area. *Figure 4* illustrates the conditioning factors used in the analysis.

Using ArcGIS 10.6.1, a series of geospatial operations were conducted to preprocess the conditioning factors. In the first stage, topographic variables were derived from the 30 m SRTM DEM. The “Slope” and “Aspect” tools were applied to generate slope and aspect layers, while the “Curvature” function was used to obtain plan curvature, distinguishing convex and concave landforms. Elevation values were extracted directly from the DEM. The SPI was calculated using *Equation 1*:

$$SPI = A_s \cdot tan(\beta) \quad \text{(Eq.1)}$$

where A_s-catchment area (m^2) and β-slope gradient in radians (Arabameri et al., 2019a; Esmali Ouri et al., 2020).

In the second stage, vegetation-related factors were prepared. The NDVI was computed from Landsat 8 OLI imagery using *Equation 2*:

$$NDVI = \frac{NIR - RED}{NIR + RED} \quad \text{(Eq.2)}$$

where NIR and RED denote the near-infrared and red spectral reflectance values, respectively (Anabitarte et al., 2020; Rouse et al., 1973). The NDVI layer was derived from cloud-free Landsat-8 OLI imagery captured on 19 April 2024, representing the early vegetation period in the study area.

LULC data were obtained from the Esri Sentinel-2 Land Cover Explorer and reclassified into major categories including water, trees, cropland, rangeland, bare land, and built-up areas. In the third stage, hydrological parameters were processed. River networks were digitized from topographic maps, after which the distance-to-river layer was generated using the “Euclidean Distance” tool (Arabameri et al., 2020a). Drainage density was determined using the “Line Density” tool, which calculates stream length per unit area (Meshram et al., 2022). All factor layers were subsequently resampled to a uniform spatial resolution of 30 m, standardized to a common coordinate system, and converted into raster format to ensure comparability across datasets. This preprocessing ensured consistency among all conditioning factors and prepared them for the subsequent erosion-susceptibility modeling.

http://www.aloki.hu ● ISSN 1589 1623 (Print) ● ISSN 1785 0037 (Online)
DOI: http://dx.doi.org/10.15666/aeer/2401_11131131

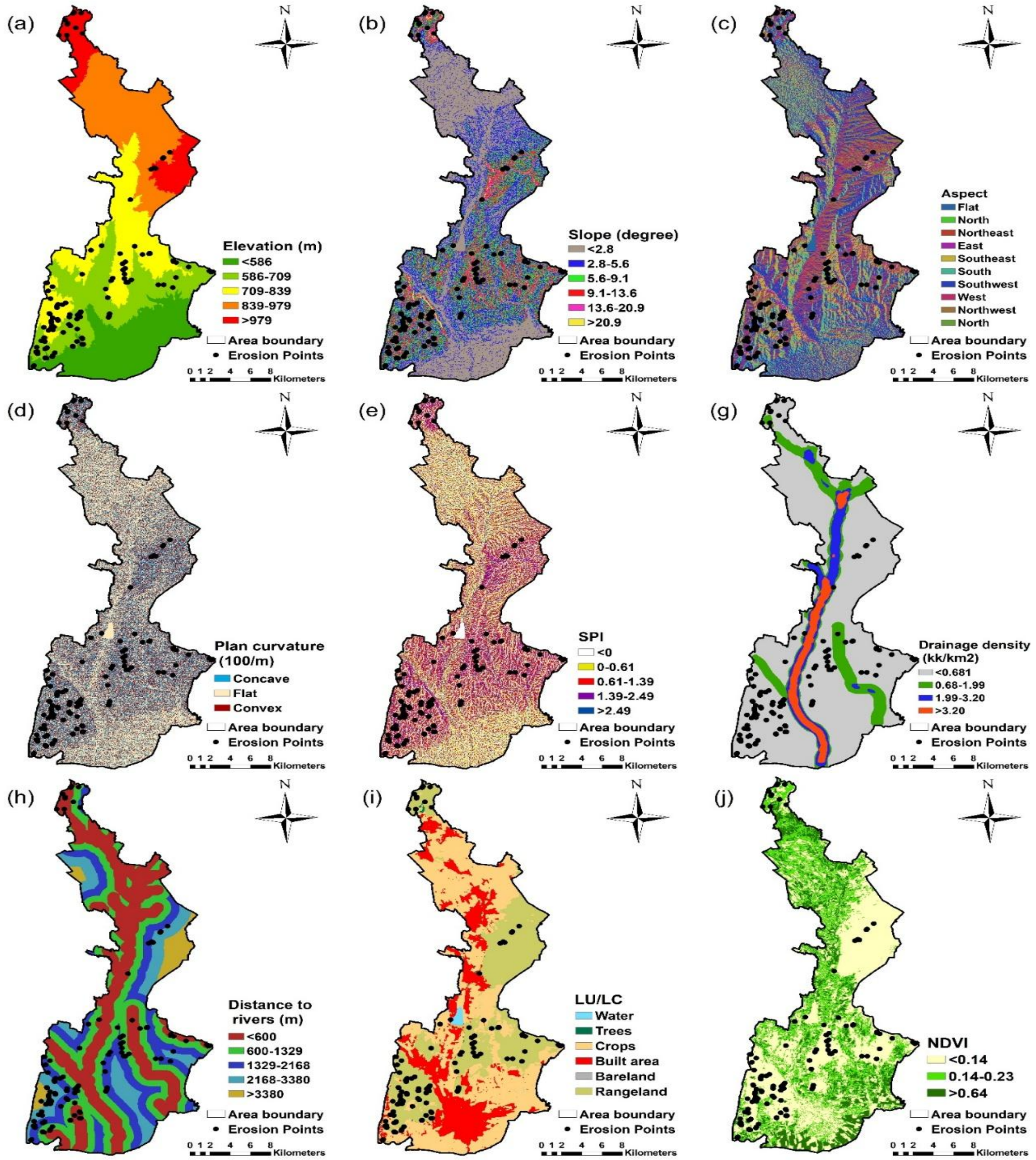

Figure 4. *Conditioning factors used for soil erosion susceptibility analysis: (a) elevation, (b) slope, (c) aspect, (d) plan curvature, (e) SPI, (g) drainage density, (h) distance to river, (i) LU/LC, (j) NDVI*

Modeling of erosion susceptibility

Three widely used bivariate statistical models FR, CF, and SI were applied to evaluate soil-erosion susceptibility. By comparing the spatial distribution of erosion occurrences with the overall distribution of each conditioning factor, these models quantify the relationship between erosion inventory points and factor classes (Azedou et al., 2021; Juliev et al., 2019; Pourghasemi et al., 2013).

Statistical Index (SI). The SI model estimates the association between erosion occurrence and factor classes by computing the natural logarithm of the ratio between the

http://www.aloki.hu ● ISSN 1589 1623 (Print) ● ISSN 1785 0037 (Online)
DOI: http://dx.doi.org/10.15666/aeer/2401_11131131

class proportion of erosion pixels and the class proportion of total pixels. Its formulation is expressed in *Equation 3*:

$$SI_i = ln\left(\frac{N_{si}/N_s}{N_{ci}/N_c}\right) \quad \text{(Eq.3)}$$

where N_{si} is the number of erosion pixels in class i, N_s- total number of erosion pixels, N_{ci} is the total number of pixels in class i, and N_c is the total number of pixels in the study area. Positive SI values indicate strong correlation between the class and erosion occurrence, while negative values suggest lower susceptibility (Juliev et al., 2019).

Frequency Ratio (FR). The FR model calculates the likelihood of erosion by comparing the proportion of erosion pixels in each class with the proportion of total pixels. The equation is given in *Equation 4*:

$$FR_i = \frac{N_{si}/N_s}{N_{ci}/N_c} \quad \text{(Eq.4)}$$

where N_{si}-number of erosion pixels in class i, N_s-total number of erosion pixels, N_{ci}-number of pixels in class i, and N_c-total number of pixels in the study area. Values of FR > 1 indicate higher susceptibility, while FR < 1 indicates lower probability (Igwe et al., 2020; Arabameri et al., 2020a).

Certainty factor (CF)

The CF model measures the degree of certainty regarding the relationship between erosion occurrence and factor classes. Its expression is shown in *Equation 5*:

$$CF_i = \begin{cases} \frac{P_a - P_s}{P_a(1 - P_s)}, if\ P_a > P_s \\ \frac{P_a - P_s}{P_s(1 - P_a)}, if\ P_a < P_s \end{cases} \quad \text{(Eq.5)}$$

where $P_a = N_{si}/N_{ci}$ is the conditional probability of erosion occurrence in class i, and $P_s = N_s/N_c$ is the prior probability of erosion occurrence in the study area. CF values range from -1 to + 1, where positive values indicate a positive correlation, and negative values indicate a negative relationship (Arabameri et al., 2019c, 2020a).

All three models were implemented in ArcGIS 10.6.1, and erosion-susceptibility maps were produced by converting factor weightings into raster layers.

Results and discussion

Conditioning factors and model outputs

Table 2 summarizes the correlation between erosion occurrences and the classes of conditioning factors and presents the statistical outputs of the three bivariate models (SI, FR, and CF). In general, croplands, built-up areas, and flat terrain classes are associated with low or negative weights. In contrast, steeper slope classes (>9.1°) and rangelands consistently exhibit high positive weights across all three models, indicating their strong contribution to erosion susceptibility. These results demonstrate that topographic characteristics and land use/land cover are the dominant factors influencing soil-erosion susceptibility in the study area.

http://www.aloki.hu ● ISSN 1589 1623 (Print) ● ISSN 1785 0037 (Online)
DOI: http://dx.doi.org/10.15666/aeer/2401_11131131

The finding that topography and land use/cover are the most influential factors in the study area is supported by the consistently high SI, FR, and CF values associated with steep slopes, low NDVI classes, and rangeland categories. Although these factors are widely acknowledged as key determinants of erosion, their dominant contribution in the Chartak district is empirically confirmed by the statistical results obtained in this study.

Table 2. *Spatial relationship between conditioning factors and erosion points analyzed using SI, FR, and CF models*

Factors	Classes	Class pixels	%Class pixels	Erosion pixels	%Erosion pixels	SI	FR	CF
Slope	<2.8	173460	39.82980599	5	3.846154	-2.57	0	-0.90
	2.8-5.6	124274	28.53573913	18	13.84615	-0.63	0.04	-0.51
	5.6-9.1	81128	906.1543617	42	32.30769	0.36	0.16	0.16
	9.1-13.6	40804	9.369395848	43	33.07692	1.40	0.33	0.26
	13.6-20.9	15837	3.636484708	22	16.92308	1.48	0.44	0.13
	>20.9	2973	0.682658902	0	0	0	0	-1
Aspect	Flat	7918	1.801752601	1	0.769231	-0.87	0.04	-0.57
	North	147	0.033450067	0	0	0	0	-1
	Northeast	8512	1.936918179	1	0.769231	0.67	0.04	-0.60
	East	31153	7.088911189	18	13.84615	0.54	0.20	0.07
	Southeast	72898	16.58804763	41	31.53846	0.65	0.20	0.17
	South	73383	16.6984101	11	8.461538	-0.45	0.05	-0.49
	Southwest	132005	30.03793283	19	14.61538	-0.74	0.05	-0.51
	West	69723	15.86557169	20	15.38462	-0.15	0.10	-0.03
	Northwest	34769	7.911737333	16	12.30769	0.36	0.16	0.04
	North	8953	2.037268381	3	2.307692	-0.30	0.12	0.002
Plan curvature	Concave	119689	26.91273357	36	27.48092	0.23	0.31	0.007
	Flat	202346	45.49861714	35	26.71756	-0.64	0.17	-0.41
	Convex	122695	27.58864929	60	45.80153	0.42	0.50	0.25
Elevation	<586	92385	20.77481971	4	3.053435	-1.93	0.02	-0.85
	586-709	100591	22.62012112	59	45.03817	0.69	0.40	0.28
	709-839	102393	23.02534085	52	39.69466	0.55	0.34	0.21
	839-979	105885	23.81059463	3	2.290076	-2.36	0.01	-0.90
	>979	43443	9.769123695	13	9.923664	0	0.20	0.001
NDVI	<0.14	234192	52.63817994	121	92.36641	0.57	0.87	0.83
	0.14-0.23	139047	31.2529079	10	7.633588	-1.53	0.12	-0.75
	>0.64	71670	16.10891216	0	0	0	0	-1
Distance to river	<600	154030	34.61091649	23	17.55725	-0.65	0.10	-0.49
	600-1329	125429	28.18420207	37	28.24427	-0.07	0.20	0.00
	1329-2168	88643	19.91829819	42	32.06107	0.51	0.32	0.15
	2168-3380	57040	12.81702705	28	21.37405	0.53	0.33	0.09
	>3380	19891	4.46955619	1	0.763359	-1.78	0.03	-0.82
LULC	Water	2289	0.514486076	0	0	0	0	-1
	Tree	827	0.18588029	0	0	0	0	-1
	Crops	198277	44.56564249	8	6.10687	-2.14	0.04	-0.86
	Build	89013	20.0069677	6	4.580153	-1.34	0.07	-0.77
	Bareland	400	0.089905824	0	0	0	0	-1
	Rangeland	154104	34.63711762	117	89.31298	0.95	0.87	0.83
SPI	<0	168791	37.93559146	48	36.64122	-0.18	0.23	-0.03
	0-0.61	84328	18.95262518	10	7.633588	-0.74	0.09	-0.59
	0.61-1.39	112643	25.31639026	61	46.56489	0.63	0.44	0.28
	1.39-2.49	59679	13.41278956	10	7.633588	-0.24	0.13	-0.43
	>2.49	19500	4.382603536	2	1.526718	-1.07	0.08	-0.65
Drainage density	<0.68	339259	76.24962916	128	97.70992	0.25	0.87	0.90
	0.68-1.99	56040	12.59518308	3	2.290076	-1.72	0.12	-0.81
	1.99-3.20	26670	5.994174391	0	0	0	0	-1
	>3.20	22963	5.161013368	0	0	0	0	-1

http://www.aloki.hu ● ISSN 1589 1623 (Print) ● ISSN 1785 0037 (Online)
DOI: http://dx.doi.org/10.15666/aeer/2401_11131131

Although positive values are intrinsic to bivariate models, comparing their magnitude and consistency provides meaningful insight. In this study, steep slopes (>9°), low NDVI classes, and rangelands exhibit consistently high positive SI, FR, and CF values, reflecting their strong contribution to erosion processes. Conversely, croplands, flat terrain, and high-NDVI areas produce negative or low weights, indicating reduced susceptibility. These patterns highlight the discriminative capabilities of the three models and their agreement with the geomorphological conditions of the study area.

The values presented in *Table 2* do not represent classical correlation coefficients but rather the bivariate association metrics (SI, FR, and CF) that quantify how strongly each factor class is linked to erosion occurrence. Positive SI values, FR > 1, or positive CF values indicate a higher likelihood of erosion within that class, while negative values indicate reduced susceptibility.

Erosion susceptibility mapping

Figure 5 illustrates the spatial distribution of erosion susceptibility generated by the FR, CF, and SI models. All three models classified the study area into five susceptibility categories: very low, low, moderate, high, and very high. Among the models, the FR model identified the largest proportion of land within the very high susceptibility zone (27.6%), while the SI model classified 17.6% of the area as very highly susceptible. The CF model produced a more balanced distribution, with 19.1% of the study area falling into the very high susceptibility class.

Area distribution by susceptibility classes

Figure 6 presents the percentage distribution of susceptibility classes for each model to further quantify the results. The SI and CF models exhibit comparatively similar patterns, particularly within the moderate and high susceptibility classes, whereas the FR model allocates a larger proportion of the study area to the very high susceptibility class. These findings highlight the sensitivity of bivariate models to the weighting strategies used in probability estimation.

Model validation

The predictive accuracy of the erosion-susceptibility maps was evaluated using the ROC-AUC. As shown in *Figure 7,* all three models achieved AUC values above 0.84, indicating reliable predictive capability. The SI (AUC = 0.879) and CF (AUC = 0.878) models produced the highest AUC values, while the FR model yielded a lower but still acceptable value (AUC = 0.843). According to the predictive power classification of Yesilnacar and Topal (2005), all three approaches fall within the range of reliable predictive performance.

Comparative performance of SI, FR and CF models

The results of the study indicate that all three statistical models SI, FR, and CF— were effective in predicting soil-erosion susceptibility in the Chartak district. The SI (AUC = 0.879) and CF (AUC = 0.878) models produced the highest AUC values, whereas the FR model yielded a lower, yet still reliable value (AUC = 0.843). Because all AUC values exceeded 0.8, each model demonstrated strong predictive capability (Arabameri et al., 2019b, 2020a). These numerical differences are consistent with

http://www.aloki.hu ● ISSN 1589 1623 (Print) ● ISSN 1785 0037 (Online)
DOI: http://dx.doi.org/10.15666/aeer/2401_11131131

previous studies; for example, Juliev (2019) reported that SI and CF often produce higher AUC values than the FR model in erosion-susceptibility assessments. The susceptibility maps produced by the three models demonstrated consistent spatial patterns. Areas characterized by low vegetation cover (NDVI < 0.14), rangelands, and steep slopes (>9°) were classified as having high or very high susceptibility. These observations align with well-established geomorphological principles: sparse vegetation provides limited protection against raindrop impact and sheet erosion, while steep terrain enhances runoff velocity (Bouamrane et al., 2024; Esmali Ouri et al., 2020). Similar to observations in earlier studies, the FR model tended to assign larger areas to the high-susceptibility class, reflecting its sensitivity to class–pixel ratios (Amare et al., 2021).

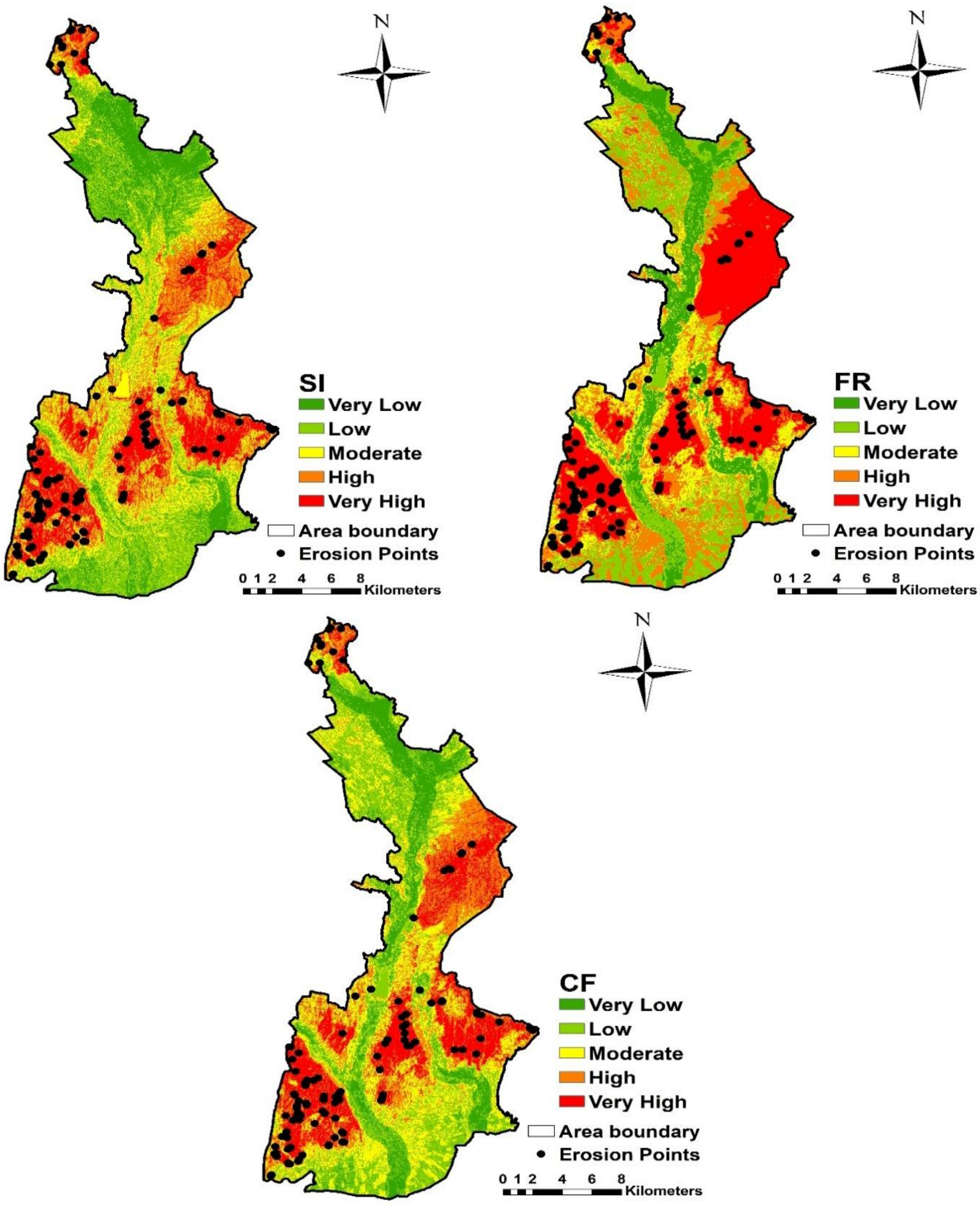

Figure 5. *Soil erosion susceptibility maps created by SI, FR and CF models*

http://www.aloki.hu ● ISSN 1589 1623 (Print) ● ISSN 1785 0037 (Online)
DOI: http://dx.doi.org/10.15666/aeer/2401_11131131

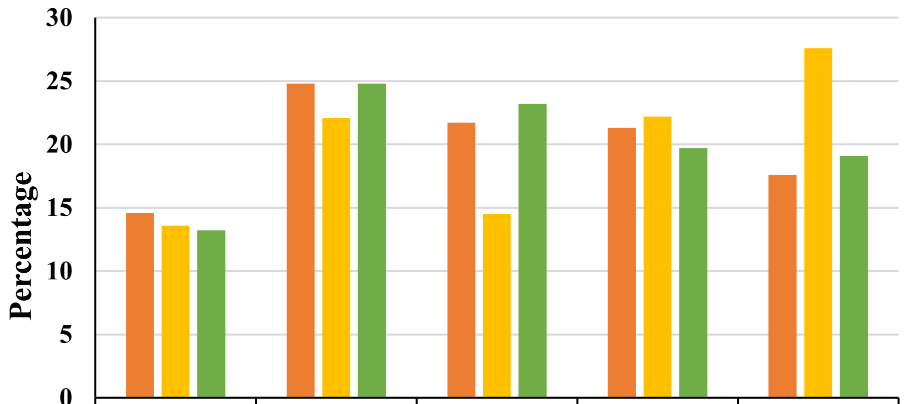

	Very low	Low	Moderate	High	Very high
SI	14.6	24.8	21.7	21.3	17.6
FR	13.6	22.1	14.5	22.2	27.6
CF	13.2	24.8	23.2	19.7	19.1

Figure 6. *Distribution of susceptibility classes (%) for SI, FR, and CF models*

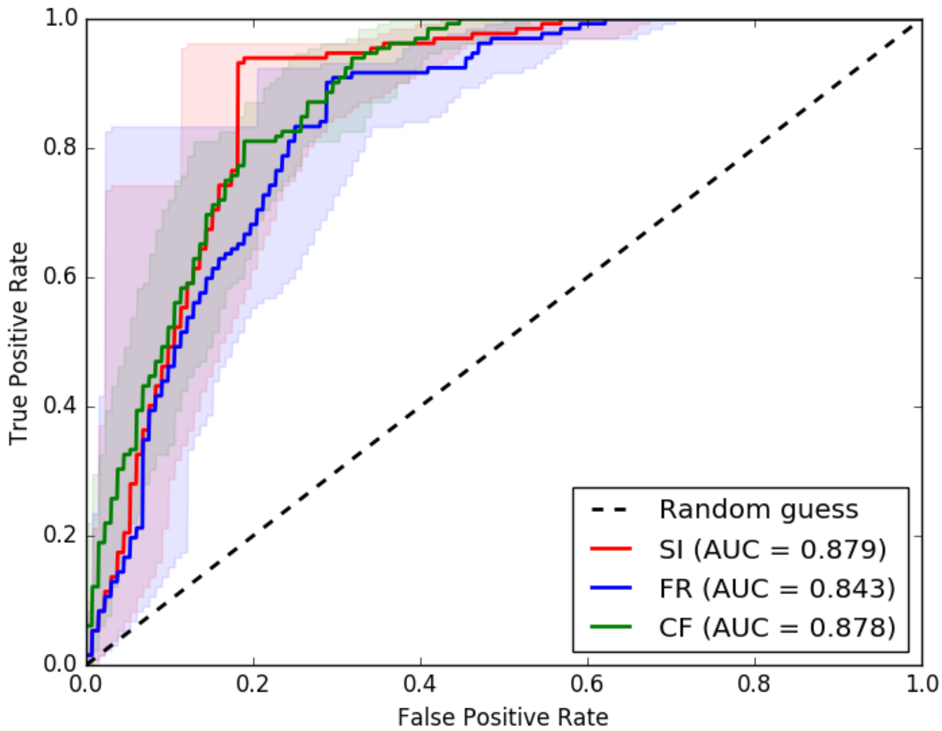

Figure 7. *ROC curve showing the predictive performance of the SI, FR, and CF models with their corresponding AUC values*

Relation to erosion research in Uzbekistan

Research on erosion in Uzbekistan has predominantly relied on empirical models such as the RUSLE. For example, Juliev (2024) conducted RUSLE-based assessments in the Ugam–Chatkal National Park, while Ibragimov et al. (2024) applied similar approaches

http://www.aloki.hu ● ISSN 1589 1623 (Print) ● ISSN 1785 0037 (Online)
DOI: http://dx.doi.org/10.15666/aeer/2401_11131131

in the Bekabad and Parkent districts. These studies primarily quantified annual soil loss and examined its relationship with land cover and topographic factors. At broader spatial scales, Chen et al. (2025) evaluated wind erosion risks in the Aral Sea basin, whereas Gafforov et al. (2020) analyzed rainfall erosivity under projected climate change in the Chirchik–Akhangaran watershed. Field-based investigations in the Namangan region (Koriyev et al., 2024b), focused on the effectiveness of terracing and mulching practices. Although these studies significantly advance erosion research in Uzbekistan, most of them emphasize basin-scale processes or annual soil-loss estimation. In contrast, the present study is the first to apply bivariate statistical modeling at the district scale in Uzbekistan. Instead of solely quantifying erosion rates, this approach identifies the probability of erosion occurrence and spatial patterns of susceptibility. Therefore, the study fills an important methodological and spatial gap, complementing existing RUSLE-based and climate-oriented assessments.

The produced susceptibility maps provide valuable decision-support information for land managers and local stakeholders. High-susceptibility zones were consistently associated with rangelands, steep slopes, and areas characterized by sparse vegetation. In these locations, soil-conservation measures such as reforestation, contour cultivation, and terracing can be strategically prioritized to effectively reduce erosion hazards and support sustainable land management. Furthermore, strengthening vegetative buffer zones along river networks may help minimize sediment transport and protect water resources. Given the increasing pressure on land resources due to population growth and climate variability in Uzbekistan, the findings offer a sound scientific basis for integrating erosion-susceptibility assessments into district-level land-use planning.

Methodological reflections and limitations

The strong performance of the SI and CF models indicates that they are suitable for data-limited environments such as Uzbekistan. Nevertheless, several limitations should be acknowledged. First, the erosion inventory relied on 133 mapped points, which although sufficient for bivariate statistical analysis may not fully represent the diversity of erosion processes, including gully development. Second, because these models depend on statistical associations between conditioning factors and documented erosion occurrences, they may not effectively capture dynamic processes such as extreme rainfall events or rapid land-use changes (Borrelli et al., 2017, 2021). Third, the tendency of the FR model to overpredict susceptibility highlights the importance of comparing multiple modeling approaches rather than relying on a single method.

Future research should explore ensemble modeling frameworks that integrate diverse machine learning and statistical techniques, including support vector machines, logistic regression, and random forests (Arabameri et al., 2019a; Esmali Ouri et al., 2020; Khosravi et al., 2023). Additionally, incorporating temporal remote-sensing datasets particularly multi-seasonal NDVI and rainfall variability may improve the representation of erosion dynamics and enhance the predictive accuracy of susceptibility assessments.

Conclusion

This study employed three bivariate statistical models SI, FR, and CF to assess soil erosion susceptibility in the Chartak district of the Namangan region. Nine conditioning factors derived from DEM, remote sensing products, and complementary datasets were used to generate susceptibility maps, which were subsequently validated using ROC-

http://www.aloki.hu ● ISSN 1589 1623 (Print) ● ISSN 1785 0037 (Online)
DOI: http://dx.doi.org/10.15666/aeer/2401_11131131

AUC metrics. The SI (0.879) and CF (0.878) models exhibited slightly higher predictive performance than the FR model (0.843), although all three achieved high accuracy values (>0.8), indicating their reliability for susceptibility assessment.

The susceptibility maps revealed that 38.9% (SI), 49.8% (FR), and 38.8% (CF) of the study area fall within high to very high susceptibility classes. Areas characterized by steep slopes, rangelands, and sparse vegetation consistently demonstrated elevated erosion susceptibility. These findings align with well-documented erosion mechanisms and, importantly, provide the first district-scale probabilistic assessment of erosion susceptibility in Uzbekistan, where such modeling approaches have not previously been applied.

The outcomes of this research have practical implications for land-use planning and soil conservation. Local authorities can use the susceptibility maps to prioritize erosion-prone zones for targeted interventions, thereby mitigating land degradation and supporting sustainable agricultural productivity. Furthermore, the methodological framework offers a replicable model for other districts in Uzbekistan and across Central Asia, expanding the range of tools available for erosion assessment beyond traditional RUSLE-based methods.

Future studies should integrate advanced machine learning algorithms and time-series datasets to further refine susceptibility mapping under changing climatic and land-use conditions. Such advancements would facilitate the development of dynamic, data-driven decision-support systems capable of informing sustainable land-management strategies at multiple administrative levels.

REFERENCES

[1] Abdikairov, B., Juliev, M., Kholmurodova, M. (2024): Analyses and assessment of soil salinity modeling: review of papers from Scopus database. – Journal of Geology, Geography and Geoecology 33(4): 647-661. https://doi.org/10.15421/112459.

[2] Akgün, A., Türk, N. (2011): Mapping erosion susceptibility by a multivariate statistical method: a case study from the Ayvalık region, NW Turkey. – Computers & Geosciences 37(9): 1515-1524. https://doi.org/10.1016/j.cageo.2010.09.006.

[3] Allafta, H., Opp, C. (2022): Soil erosion assessment using the RUSLE model, remote sensing, and GIS in the Shatt Al-Arab Basin (Iraq-Iran). – Applied Sciences 12(15): 7776. https://doi.org/10.3390/app12157776.

[4] Amare, S., Langendoen, E., Keesstra, S., Ploeg, M., Gelagay, H., Lemma, H., Zee, S. (2021): Susceptibility to gully erosion: applying random forest (RF) and frequency ratio (FR) approaches to a small catchment in Ethiopia. – Water 13(2): 216. https://doi.org/10.3390/w13020216.

[5] Anabitarte, A., Subiza-Pérez, M., Ibarluzea, J., Azkona, K., García-Baquero, G., Miralles-Guasch, C., Irazusta, J., Whitworth, K. W., Vich, G., Lertxundi, A. (2020): Testing the multiple pathways of residential greenness to pregnancy outcomes model in a sample of pregnant women in the metropolitan area of Donostia-San Sebastián. – International Journal of Environmental Research and Public Health 17(12): 4520. https://doi.org/10.3390/ijerph17124520.

[6] Arabameri, A., Rezaei, K., Pourghasemi, H. R., Lee, S., Yamani, M. (2018): GIS-based gully erosion susceptibility mapping: a comparison among three data-driven models and AHP knowledge-based technique. – Environmental Earth Sciences 77(17): 628. https://doi.org/10.1007/s12665-018-7808-5.

[7] Arabameri, A., Cerda, A., Tiefenbacher, J. P. (2019a): Spatial pattern analysis and prediction of gully erosion using novel hybrid model of entropy-weight of evidence. – Water 11(6): 1129. https://doi.org/10.3390/w11061129.

[8] Arabameri, A., Pradhan, B., Lombardo, L. (2019b): Comparative assessment using boosted regression trees, binary logistic regression, frequency ratio and numerical risk factor for gully erosion susceptibility modelling. – Catena 183: 104223. https://doi.org/10.1016/j.catena.2019.104223.

[9] Arabameri, A., Pradhan, B., Rezaei, K. (2019c): Gully erosion zonation mapping using integrated geographically weighted regression with certainty factor and random forest models in GIS. – Journal of Environmental Management 232: 928-942. https://doi.org/10.1016/j.jenvman.2018.11.110.

[10] Arabameri, A., Pradhan, B., Bui, D. T. (2020a): Spatial modelling of gully erosion in the Ardib River Watershed using three statistical-based techniques. – Catena 190: 104545. https://doi.org/10.1016/j.catena.2020.104545.

[11] Arabameri, A., Cerda, A., Pradhan, B., Tiefenbacher, J. P., Lombardo, L., Bui, D. T. (2020b): A methodological comparison of head-cut based gully erosion susceptibility models: combined use of statistical and artificial intelligence. – Geomorphology 359: 107136. https://doi.org/10.1016/j.geomorph.2020.107136.

[12] Arabameri, A., Rezaie, F., Pal, S. C., Cerda, A., Saha, A., Chakrabortty, R., Lee, S. (2021): Modelling of piping collapses and gully headcut landforms: evaluating topographic variables from different types of DEM. – Geoscience Frontiers 12(6): Article 6. https://doi.org/10.1016/j.gsf.2021.101230.

[13] Azedou, A., Lahssini, S., Khattabi, A., Meliho, M., Rifai, N. (2021): A methodological comparison of three models for gully erosion susceptibility mapping in the rural municipality of El Faid (Morocco). – Sustainability 13(2): 682. https://doi.org/10.3390/su13020682.

[14] Borges Neto, I. D. O., Xavier, R. A., De Souza, B. I., Santos, L. J. C., Soares, D. A., De Souza, J. J. L. L. (2023): Preliminary experimental data on surface runoff and soil loss in the Caatinga. – Earth Surface Processes and Landforms 48(9): 1712-1723. https://doi.org/10.1002/esp.5581.

[15] Borrelli, P., Robinson, D. A., Fleischer, L. R., Lugato, E., Ballabio, C., Alewell, C., Meusburger, K., Modugno, S., Schütt, B., Ferro, V., Bagarello, V., Oost, K. V., Montanarella, L., Panagos, P. (2017): An assessment of the global impact of 21st century land use change on soil erosion. – Nature Communications 8(1): 2013. https://doi.org/10.1038/s41467-017-02142-7.

[16] Borrelli, P., Alewell, C., Alvarez, P., Anache, J. A. A., Baartman, J., Ballabio, C., Bezak, N., Biddoccu, M., Cerdà, A., Chalise, D., Chen, S., Chen, W., De Girolamo, A. M., Gessesse, G. D., Deumlich, D., Diodato, N., Efthimiou, N., Erpul, G., Fiener, P., et al. (2021): Soil erosion modelling: a global review and statistical analysis. – Science of the Total Environment 780: 146494. https://doi.org/10.1016/j.scitotenv.2021.146494.

[17] Bouamrane, A., Boutaghane, H., Bouamrane, A., Dahri, N., Abida, H., Saber, M., Kantoush, S. A., Sumi, T. (2024): Soil erosion susceptibility prediction using ensemble hybrid models with multicriteria decision-making analysis: case study of the Medjerda basin, northern Africa. – International Journal of Sediment Research 39(6): 998-1014. https://doi.org/10.1016/j.ijsrc.2024.08.003.

[18] Cao, X., Cheng, Y., Jiao, J., Jian, J., Bai, L., Li, J., Ma, X. (2023): Impact of land use/cover changes on soil erosion by wind and water from 2000 to 2018 in the Qaidam Basin. – Land 12(10): 1866. https://doi.org/10.3390/land12101866.

[19] Chen, Z., Gao, X., Lei, J. (2025): Monitoring of wind erosion in the southern Aral Sea using SBAS-InSAR technology. – International Soil and Water Conservation Research 13: 551-563. https://doi.org/10.1016/j.iswcr.2025.05.005.

[20] David Raj, A., Kumar, S., Sooryamol, K. R., Sankar, M., George K., J. (2025): Assessment of soil erosion rates, carbon stocks, and erosion-induced carbon loss in dominant forest types of the Himalayan region using fallout-137Cs. – Scientific Reports 15(1): 14950. https://doi.org/10.1038/s41598-025-94953-8.

[21] Djanpulatova, Z. A., Juliev, M. K., Abdikairov, B. E., Kholmurodova, M. D., Turdalieva, S. R., Khadjieva, Z. B. (2025): Ecosystem services in achieving SDGs: a bibliometric overview 2015-2024. – Applied Ecology and Environmental Research 23(4): 6223-6246. https://doi.org/10.15666/aeer/2304_62236246.
[22] Dou, X., Ma, X., Zhao, C., Li, J., Yan, Y., Zhu, J. (2022): Risk assessment of soil erosion in Central Asia under global warming. – Catena 212. https://doi.org/10.1016/j.catena.2022.106056.
[23] Esmali Ouri, A., Golshan, M., Janizadeh, S., Cerdà, A., Melesse, A. M. (2020): Soil erosion susceptibility mapping in Kozetopraghi catchment, Iran: a mixed approach using rainfall simulator and data mining techniques. – Land 9(10): 368. https://doi.org/10.3390/land9100368.
[24] Gafforov, K. Sh., Bao, A., Rakhimov, S., Liu, T., Abdullaev, F., Jiang, L., Durdiev, K., Duulatov, E., Rakhimova, M., Mukanov, Y. (2020): The assessment of climate change on rainfall-runoff erosivity in the Chirchik–Akhangaran Basin, Uzbekistan. – Sustainability 12(8): 3369. https://doi.org/10.3390/su12083369.
[25] Gafurova, L., Juliev, M. (2021): Soil Degradation Problems and Foreseen Solutions in Uzbekistan. – In: Dent, D., Boincean, B. (eds.) Regenerative Agriculture. Springer International Publishing, Cham, pp. 59-67. https://doi.org/10.1007/978-3-030-72224-1_5.
[26] Ibragimov, O., Inamov, B., Alimakhamatova, S. (2024): Assessing soil erosion dynamics in the Bekabad district, Uzbekistan: a remote sensing approach integrating the RUSLE model and Google Earth engine. – E3S Web of Conferences 590: 01005. https://doi.org/10.1051/e3sconf/202459001005.
[27] Igwe, O., John, U. I., Solomon, O., Obinna, O. (2020): GIS-based gully erosion susceptibility modeling, adapting bivariate statistical method and AHP approach in Gombe town and environs Northeast Nigeria. – Geoenvironmental Disasters 7(1): 32. https://doi.org/10.1186/s40677-020-00166-8.
[28] Juliev, M., Mergili, M., Mondal, I., Nurtaev, B., Pulatov, A., Hübl, J. (2019): Comparative analysis of statistical methods for landslide susceptibility mapping in the Bostanlik District, Uzbekistan. – Science of the Total Environment 653: 801-814. https://doi.org/10.1016/j.scitotenv.2018.10.431.
[29] Juliev, M., Gafurova, L., Ergasheva, O., Ashirov, M., Khoshjanova, K., Mirusmanov, M. (2022): Land Degradation Issues in Uzbekistan. – In: Al-Quraishi, A. M. F., Mustafa, Y. T., Negm, A. M. (eds.) Environmental Degradation in Asia. Springer International Publishing, Cham, pp. 163-176. https://doi.org/10.1007/978-3-031-12112-8_8.
[30] Juliev, M., Kholmurodova, M., Abdikairov, B., Abuduwaili, J. (2024a): A comprehensive review of soil erosion research in Central Asian countries (1993-2022) based on the Scopus database. – Soil and Water Research 19(4): 244-256. https://doi.org/10.17221/82/2024-SWR.
[31] Juliev, M., Kholmurodova, M., Gafurova, L., Khoshjanova, K., Khomidov, A., Agzamova, I., Normatova, N., Gulyamov, G., Muratova, M., Gulamkadirova, M. (2024b): Modeling of soil erosion based on geospatial techniques and the RUSLE model for the Ugam Chatkal National Park, Uzbekistan. – Journal of Geology, Geography and Geoecology 33(3): 485-494. https://doi.org/10.15421/112445.
[32] Kanianska, R., Kizeková, M., Jančová, Ľ., Čunderlík, J., Dugátová, Z. (2024): Effect of soil erosion on soil and plant properties with a consequence on related ecosystem services. – Sustainability 16(16): 7037. https://doi.org/10.3390/su16167037.
[33] Kholdorov, S., Jabbarov, Z., Shamsiddinov, T. (2023): Soil governance: a review of the current legislative framework for managing soil resources in Uzbekistan. – Soil Security 13: 100105. https://doi.org/10.1016/j.soisec.2023.100105.
[34] Kholmurodova, M., Juliev, M., Abdikairov, B., Djanpulatova, Z., Turdalieva, S., Khadjieva, Z., Khamidullaev, Sh., Shamsiev, M. (2025a): A systematic review of soil erosion susceptibility: trends and insights from 2010 to 2023. – Applied Ecology and Environmental Research 23(5): 9991-10013.

https://doi.org/10.15666/aeer/2305_999110013.
[35] Kholmurodova, M., Juliev, M., Bakhodirova, Sh., Abdikairov, B., Israilov, I., Rashidov, Ja. (2025b): Global research trends on RUSLE model: bibliometric analysis using R Biblioshiny and VOSviewer. – Dokuchaev Soil Bulletin 125: 293-327. https://doi.org/10.19047/0136-1694-2025-125-293-327.
[36] Khosravi, K., Rezaie, F., Cooper, J. R., Kalantari, Z., Abolfathi, S., Hatamiafkoueieh, J. (2023): Soil water erosion susceptibility assessment using deep learning algorithms. – Journal of Hydrology 618: 129229. https://doi.org/10.1016/j.jhydrol.2023.129229.
[37] Koriyev, M., Fonseka, P. U., Umurzakova, U. N., Rozumbetov, K. U., Arachchi, S. M. A., Erkudov, V. O., Mehta, D. J., Rathnayake, U. S. (2024a): Soil salinity status in Namangan Region, Uzbekistan. – Suranaree Journal of Science and Technology 31(5): 1-15. https://doi.org/10.55766/sujst-2024-05-e05652.
[38] Koriyev, M., Rahimov, A., Toshmirzaeva, G., Umurzakova, U., Juraev, Z. (2024b): A case study on terracing and mulching in Namangan region hills located in Uzbekistan. – Journal of Applied and Natural Science 16(4): 1830-1841. https://doi.org/10.31018/jans.v16i4.6147.
[39] Meliho, M., Khattabi, A., Mhammdi, N. (2018): A GIS-based approach for gully erosion susceptibility modelling using bivariate statistics methods in the Ourika watershed, Morocco. – Environmental Earth Sciences 77(18): 655. https://doi.org/10.1007/s12665-018-7844-1.
[40] Meshram, S. G., Singh, V. P., Kahya, E., Sepehri, M., Meshram, C., Hasan, M. A., Islam, S., Duc, P. A. (2022): Assessing erosion prone areas in a watershed using interval rough-analytical hierarchy process (IR-AHP) and fuzzy logic (FL). – Stochastic Environmental Research and Risk Assessment 36(2): 297-312. https://doi.org/10.1007/s00477-021-02134-6.
[41] Montanarella, L., Pennock, D. J., McKenzie, N., Badraoui, M., Chude, V., Baptista, I., Mamo, T., Yemefack, M., Singh Aulakh, M., Yagi, K., Young Hong, S., Vijarnsorn, P., Zhang, G.-L., Arrouays, D., Black, H., Krasilnikov, P., Sobocká, J., Alegre, J., Henriquez, C. R., et al. (2016): World's soils are under threat. – Soil 2(1): 1. https://doi.org/10.5194/soil-2-79-2016.
[42] Pourghasemi, H. R., Pradhan, B., Gokceoglu, C., Mohammadi, M., Moradi, H. R. (2013): Application of weights-of-evidence and certainty factor models and their comparison in landslide susceptibility mapping at Haraz watershed, Iran. – Arabian Journal of Geosciences 6(7): 2351-2365. https://doi.org/10.1007/s12517-012-0532-7.
[43] Raza, A., Vianna, M. D. S., Ahmadi, S. H., Habib-ur-Rahman, M., Gaiser, T. (2024): Comparison of predictive modeling approaches to estimate soil erosion under spatially heterogeneous field conditions. – Environmental Modelling & Software 180: 106145. https://doi.org/10.1016/j.envsoft.2024.106145.
[44] Rouse, J. W., Haas, R. H., Schell, J. A., Deering, D. W. (1973): Monitoring Vegetation Systems in the Great Plains with ERTS: Vol. SP-351. – NASA, Greenbelt, MD.
[45] Rustamjonovich, K. M. (2019): Geoecological issues of horticulture development in the foothills of the Namangan region of the Republic of Uzbekistan. – Indonesian Journal of Innovation Studies 5. https://doi.org/10.21070/ijins.v7i0.34.
[46] Samuel, K. J., Durowoju, O. S., Ayeni, 'Bola, Adelabu, S. A., Chigbundu, O. S. (2025): Geospatial analysis of soil erosion and implications for sustainable development goals in tropical ecological zones. – Discover Environment 3(1): 14. https://doi.org/10.1007/s44274-025-00198-7.
[47] Sanakulov, S. F., Turdaliev, J. M., Bakhodirov, Z., Sodikova, G. S. (2023): Evaluation of Fertility of Irrigated Soils in Uzbekistan. – In: Kodirova, D. (ed.) E3S Web of Conferences Vol. 421. EDP Sciences. https://doi.org/10.1051/e3sconf/202342101002.
[48] Schmidt, J. (Ed.). (2000): Soil Erosion. – Springer, Berlin. https://doi.org/10.1007/978-3-662-04295-3.

[49] Sodikova, G., Shamsiddinov, T., Shadieva, N., Usmonova, M. (2025): GIS assessment of soil erosion in Uzbekistan's rainfed mountain lands. – BIO Web of Conferences 173: 03024. https://doi.org/10.1051/bioconf/202517303024.
[50] Vaezi, A. R., Sahandi, K. (2024): Introducing dryland furrow soil erosion; a new form of water erosion and investigating the dependency on soil properties in the semi-arid regions, NW Iran. – Catena 243: 108154. https://doi.org/10.1016/j.catena.2024.108154.
[51] Wang, Y., Zhang, Y., Chen, H. (2023): Gully erosion susceptibility prediction in Mollisols using machine learning models. – Journal of Soil and Water Conservation 78(5): 385-396. https://doi.org/10.2489/jswc.2023.00019.
[52] Wang, Y., Sun, X., Miao, L., Wang, H., Wu, L., Shi, W., Kawasaki, S. (2024): State-of-the-art review of soil erosion control by MICP and EICP techniques: problems, applications, and prospects. – Science of The Total Environment 912: 169016. https://doi.org/10.1016/j.scitotenv.2023.169016.
[53] World Bank (2019): Environmental and Social Management Framework: Uzbekistan. – World Bank, Washington, DC. https://documents1.worldbank.org/curated/en/101551567745588689.
[54] Yesilnacar, E., Topal, T. (2005): Landslide susceptibility mapping: a comparison of logistic regression and neural networks methods in a medium scale study, Hendek region (Turkey). – Engineering Geology 79(3-4): 251-266. https://doi.org/10.1016/j.enggeo.2005.02.002.
[55] Zachar, D. (1982): Soil Erosion. – Elsevier, Amsterdam.

http://www.aloki.hu ● ISSN 1589 1623 (Print) ● ISSN 1785 0037 (Online)
DOI: http://dx.doi.org/10.15666/aeer/2401_11131131